Available online at **www.joac.info**

ISSN: 2278-1862

Journal of Applicable Chemistry

2019, 8 (1): 389-402

(International Peer Reviewed Journal)

Aqueous Phase Removal of Phenol using Thermally Activated *Xanthium strumarium* Bioadsorbent

Rohit Verma[1]*, Man Mohan S. Jassal[2] and Vipin K. Saini[3]

1. Department of Chemistry, Government (PG) College, Gopeshwar, Chamoli, Uttarakhand-246401, **INDIA**
2. Department of Chemistry, D. A. V. (PG) College, Dehradun, Uttarakhand-248001, **INDIA**
3. School of Environmental Science, Doon University, Dehradun, Uttarakhand, **INDIA**

Email: rohitv198@gmail.com

Accepted on 17th January, 2019

ABSTRACT

Phenol and its derivates are carcinogenic and harmful pollutants due to stability and persistence nature. Besides other methods bio-adsorption is found to be efficient and economical way to removal phenolic pollutants from their aqueous phase. In this study, thermally activated Xanthium strumarium based bio-adsorbent is developed and characterized by BET, SEM, FTIR, XRD and pH_{ZPC} methods. These studies confirm highly microporous nature along with basic surface of the bioadsorbent. The adsorption analysis is done attain optimum contact time, pH and the dependence of adsorption capacity on initial concentration and temperature. The contact time and optimum pH of the adsorption of phenol is found to 30 minutes and pH 7, respectively. The adsorption capacity of phenol on XPT1 is found to increase with increases in initial concentration and it decreases with increase in temperature. The adsorption isotherm modelling is found to be well fitted with Langmuir model at all temperatures, suggesting chemical interactions between phenol and XPT1 adsorbent.

Graphical Abstract

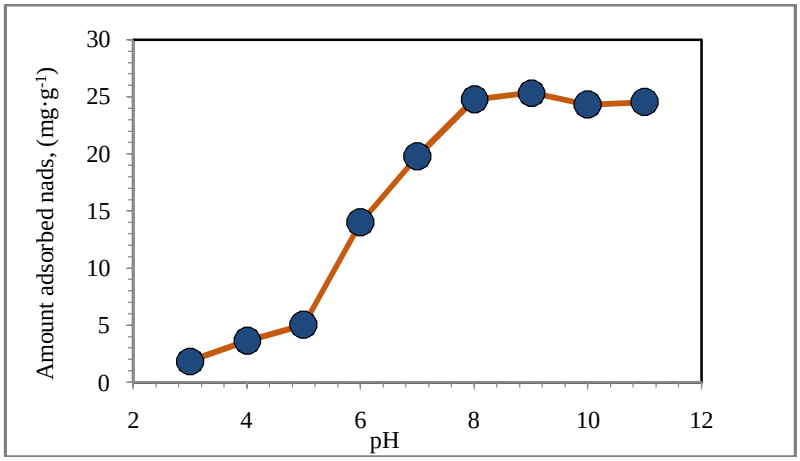

Variation of Adsorption capacity with pH for Phenol on XPT1.

Keywords: Phenol, Xanthium Strumarium, Aqueous phase, Bioadsorption, Langmuir isotherm.

INTRODUCTION

Phenolic compounds commonly have hydroxyl group directly attached with aromatic ring, beside other linked groups like methyl, halogens, nitro, etc. The phenols, chlorophenols, cresols, nitrophenols are important phenolic compounds, used in various procedures in chemical, pharmaceutical, petrochemical, paper, wood, dye and pesticide based industries [**1**]. The phenolic compounds are present in the coal-coking, synthetic rubber [**2**], leather, olive oil [**3**], phenol production [**4**] based industrial wastewater. The chlorophenols are priority pollutants due to toxic and resistance to microbial degradation, leading to their accumulation in food chain [**5**]. The permissible limits for phenolic presence in water are 0.1 mg L^{-1} as per US Environment Protection Agency (USEPA), and about 1.0 µg L^{-1} according to Bureau of Indian Standards (BIS) [**6**]. The major adverse human and environmental impacts of phenolic compounds includes loss of aquatic life, inhibition of microbial community, carcinogenicity to animals [**1**], liver damage, diarrhoea, mouth ulcers and haemolytic anaemia in humans on low phenolic water consumption [**6**]. The long term exposure to phenolic concentration over 2 mg L^{-1} are toxic to fish and concentrations between 10 and 100 mg L^{-1} result in death of aquatic life [**7**].

The contemporary methods of removal of phenolic compounds includes physical treatment methods like activated carbon adsorption, hyper-filtration, solvent extraction, reverse osmosis, etc; chemical treatment methods like chemical oxidation, incineration, chemical degradation, wet oxidation, hypercritical oxidation, UV/H_2O_2 method, TiO_2 photochemical oxidation, high-pressure impulsive discharge, low temperature plasma, high frequency ultrasonic method, etc; biological treatment methods like activated sludge, membrane separation technique, aerobic/anaerobic method, etc [**5**]. The physical and chemical methods are associated with high cost and economically not viable, whereas biological methods are associated with efficiency issues, especially when phenolic compounds are in traces.

Traditionally activated carbon adsorption method in removal of phenolic derivatives is found to be most effective, but it is expensive in comparison to other methods [**3, 8, 9**]. That is why many alternate and cheaper forms of adsorbents have been developed in recent time, such as activated carbon fiber [**1**], fungal biomass [**2**], sludge [**5**], clay [**4**] agricultural waste [**6**], etc. The activated carbon developed from any biological source is known as bioadsorbent, the examples include agricultural waste, animal waste, human waste etc. Bioadsorption is the utilization of such waste after physical or chemical treatment in pollutant removal from waste water. The bioadsorbent efficiency is dependent on the pH, temperature, contact time, adsorbent dose and pollutant initial concentration. The pollutant binding to the bioadsorbent is function of nature of surface groups, pores structure, and particle size of the adsorbent.

Bioadsorption is a promising method in pollutant removal including phenols in their aqueous phase. The importance of bioadsorbent lies in the fact that this method is highly selective, cost effective and highly removal efficiency [**5**]. The bioadsorbents has been prepared from weed plants such as Alligator weed [**11**], *Lantana camara* [**12**], *Xanthium strumarium* [**13, 14**]. The plant based adsorbents are economical, renewable, abundant and are mainly composed of cellulose and lignin hence can be converted to possible bioadsorbents. The plant biomasses utilized by various researchers are modified forms of seed, leaf, root, bark and peel [**15**]. The bioadsorption method can be utilized to accumulate phenols, chlorophenols, nitrophenols and related compounds from wastewater. The plant weed based bioadsorbent is abundant and reduce the removal cost to greater levels.

The present work is focused on development of more economical, efficient and easily available *Xanthium strumarium* derived adsorbent. The powdered seeds were used to prepare activated carbon by thermal activation. The developed activated carbon was characterized by its structure and surface properties. The thermally activated biomass was investigated for their phenol removal capacity by batch experiments. The isotherm modelling was applied to get insight of adsorption behavior of these

materials. To the best of our knowledge, this study is the first study where *Xanthium* based bioadsorbent is used in phenolic removal.

MATERIALS AND METHODS

Materials: The chemicals used in this work were of analytical grade and were purchased from Hi Media (India). The deionized water was used in preparations of solutions. Analytical grade Phenol was used to prepare respective aqueous solution. The temperature conditions are specified in each experiment. The structural and molecular properties of phenol [**1, 16**] are presented in table 1.

Table 1. Structural and molecular properties of phenol

Phenolic Compound	Molecular Structure	Molecular Weight ($g.mol^{-1}$)	Boiling Point (°C)	pK_a at 25°C	Aqueous Solubility at 25°C ($g\ L^{-1}$)	Maximum wavelength, λ_{max} (nm)
Phenol	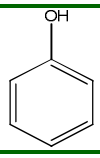	94	182	9.99	93	270

Adsorbent preparation: The seeds of *Xanthium strumarium* were collected from Manduwala region of Dehradun, Uttarakhand. The properly washed samples are dried in hot air oven for 4 h at 100°C. In thermal activation, the methodology was adopted from literature [**3, 6, 17,** and **18**]. The pre-treated biomass is thermally converted to bioadsorbents *Xanthium*-Physically-Thermally (activated), XPT under the following temperature and time conditions: XPT1, 600°C, 5 h, XPT2, 500°C, 5 h, XPT3, 400°C, 5 h. These prepared samples of XPT were placed in desiccators in dark until required.

Adsorption characterization: The surface morphology was observed by scanning electron microscopy (SEM) using ZEISS EVO Series Microscope EVO 50. In order to assess the nature of surface functional groups, Fourier transform infrared analysis was done using FTIR Model 7000 (Varian). The BET surface areas of the bioadsorbent developed were determined by liquid nitrogen adsorption method at 77K using Micrometrics ASAP 2020. The amorphous or crystalline nature of the bioadsorbent was analyzed using a powdered XRD diffractometer (model X'Pert PRO, Panalytical) using Cu-Kα radiation (λ=1.54 Å) at 45 KV and 40 mA. Scanning is performed in the range of 10 to 90° with a scan speed of 2° min^{-1}. The elemental analysis was performed by CHNS model number EA 3000, serial number 8154, Euro. The surface charge of the bioadsorbent was determined by pH_{ZPC}, according to methodology used in [**19**].

Adsorption studies: The adsorption properties of adsorbent are influenced by various factors, like time, pH, temperature and adsorbate (phenolic) concentration. Thus variation in adsorption is studied with variation in these parameters. The effect of concentration, pH and temperature were performed in terms of batch experiments. The samples obtained from batch experiments were filtered using Millipore Millex HN Syringe Filter with Nylon Membrane (0.45 microns). The filtered solutions were analysed by Thermo Scientific Evolution 201 UV-Visible spectrophotometer. The mass balance equation was used in calculation of adsorbed amount of phenol and chlorophenols.

$$q_e = \left(\frac{Co - Cc}{m \times 1000}\right) V \qquad (1)$$

Where q_e is the amount adsorbed ($mg\ g^{-1}$), C_o and C_e are the initial and equilibrium concentrations ($mg\ L^{-1}$), m is the mass (g) of adsorbent used and V is volume (mLl) of the adsorbate solution.

Phenol was adsorbed on developed bioadsorbents at 30°C (± 2°C) along with 40°C and 50°C (in study of effect of temperature). The solutions of known concentrations (known as initial concentration, which is variable particularly in the experiment of effect of concentration) and volume (250 mL) were taken in Erlenmeyer flask (250 mL), stirred with a fixed biosorbent dose (2 gm L^{-1}), in a temperature controlled magnetic stirrer. The Erlenmeyer flask were tightly stoppered to avoid any loss of adsorbate or solvent (by vaporization) and to avoid any interference from outer environment. The concentration of the adsorbate in the residual solution (final concentration, c_c) was measured by using UV-Visible spectrophotometer at λ_{max} 270 nm for phenol. The reproducibility in concentration determination was confirmed by repeating the experiments at least three times under same conditions and average values are reported. The standard deviations were within the range of ± 4.8%. The error bars in calculations and in figures were smaller in magnitude and therefore not shown.

The amount of adsorbates adsorbed was determined by using equation (1). The pH of the solutions was adjusted by using 0.1N NaOH and 0.1N HCl solutions. The pH of the solutions was measured before and after the equilibrium and any slight change in pH was observed.

Adsorption isotherms: The adsorption isotherms are used to analyze the adsorption capacity in terms of adsorbate-adsorbent interaction. These isotherms gives certain constants, which describes the mathematical relationship between quantities of adsorbate adsorbed per unit mass of adsorbent and the equilibrium concentration of adsorbate in the solution. In this study the solutions of phenol (250 mL) of different concentrations in the range of 20 to 200 mg L^{-1} were stirred with 0.5 g of adsorbent to attain equilibrium, after which the samples are filtered and analyzed by UV-Vis spectrophotometer to determine the C_e and q_e. The adsorption isotherms for adsorbate-adsorbent were obtained by plotting q_e as a function C_e. The different mathematical models were applied to these isotherms and compared for better fitting [20]. In this study the nonlinear Langmuir (2) and Freundlich (3) models were fitted with C_e and q_e.

$$q_e = \frac{q_{max}.b.C_e}{1+bC_e} \quad (2)$$

$$q_e = K_f.{C_e}^{1/n} \quad (3)$$

In equation (2) 'q_{max}' and 'b' are the Langmuir constants that denote maximum adsorption potential and equilibrium constant. Similarly 'K_f' and 'n' are the Freundlich constant in equation (3), showing adsorption capacity and adsorption intensity, respectively.

RESULTS AND DISCUSSION

Physical characterization of activated carbon: The pore size and pore distribution primarily determine the surface area and thus adsorption properties of activated carbons [22].The porosity and surface area of the developed activated carbon samples from *Xanthium strumarium* were assessed by nitrogen adsorption at -196°C, as presented in table 2. The *Xanthium strumarium* seed biomass has higher cellulose content, as in apricot stones and almond shells, and thereby has greater micropore-proportion [23]. The limiting adsorption of the adsorbate is function of accessible micropore volume, and quite independent of the internal surface area. Thermal treatment above 400°C causes enhancement in surface area, mainly due to opening of restricted pores and formation of new micropores [17]. This suggests XPT1 has greater micropore-proportion, leading to greater surface area and higher adsorption, as compared to XPT2 and XPT3. The proportion of micropore (pores with pore diameter lesser than 2 nm) volume for XPT1 is much higher as compared to other XPT2 and XPT3 samples, as shown in figure 1. In figure 2 on increasing activation temperature there is a quantitative rise in the pore volume ($cm^3\ g^{-1}$. Angstrom) along with the shift in maxima towards 5 nm. The other consistent observation from the figure 1 and 2 is the rise in mesopores-proportion relative to that of micropores. This is attributed to enlargement of micropores due to burn-off and consequently gasification process at elevated temperatures [16].

Table 2. Details of BET surface area, Langmuir surface area, pore volume and pore size for Untreated *Xanthium*, and bioadsorbent developed

Sample	BET surface area (XPT1)	Langmuir surface area (in $m^2 g^{-1}$)	Total Pore volume (in $cm^2 g^{-1}$)	Adsorption average pore width (in nm)	Average Particle size (in nm)
Untreated powdered *Xanthium*	366.4	2220.09	0.365678	3.99	16.37
XPT3	406.09	11835.05	0.368938	3.63	14.77
XPT2	792.81	47518.04	0.727470	3.67	7.56
XPT1	1352.82	114153.08	1.199014	3.54	4.43

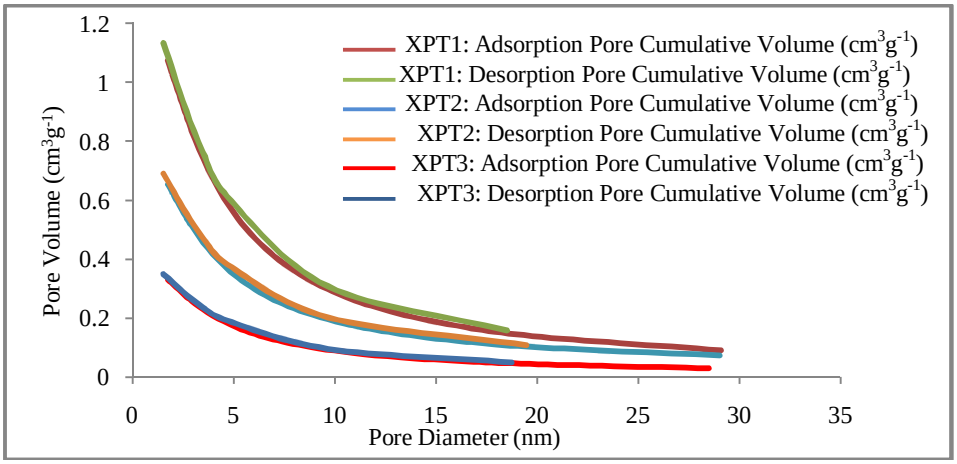

Figure 1. Pore Cumulative Volume ($cm^3 g^{-1}$) Vs Pore Diameter (nm) low-temperature nitrogen adsorption isotherms, at -196°C, for XPT1, XPT2 and XPT3 samples.

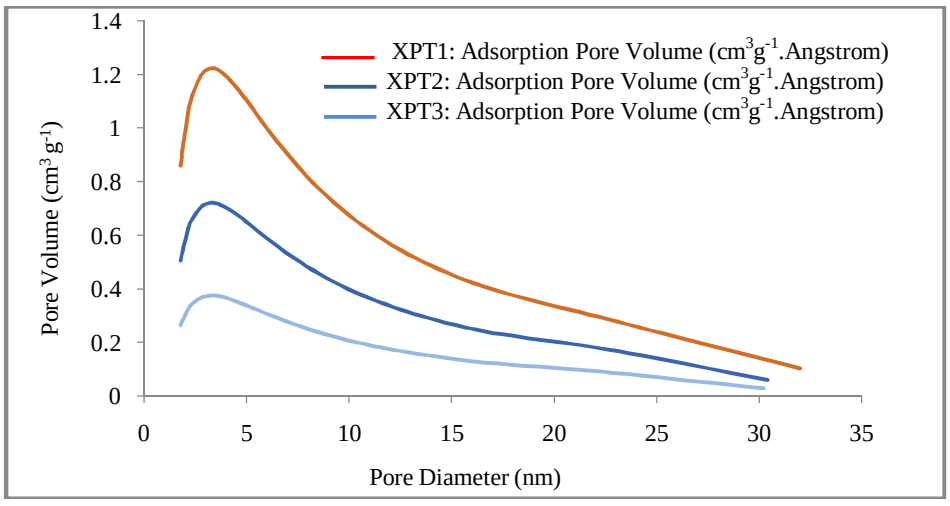

Figure 2. Pore Volume ($cm^3 g^{-1}$, Angstrom) Vs Pore Diameter (nm) low-temperature nitrogen adsorption isotherms, at -196°C, for XPT1, XPT2 and XPT3 samples.

The parameters such as BET surface area, Langmuir Surface area, total pore volume, adsorption average pore width and average particle size for untreated *Xanthium*, XPT1, XPT2 and XPT3 has been compared in table 3. The steady variation in these parameters suggests that the BET and Langmuir surface area increases with the temperature of activation. The activation increased the total pore volume 2.5 times in XPT1 as compared to untreated *Xanthium*. The average particle size has been decreased in XPT1 to almost one-fourth of that in the untreated *Xanthium*. The average pore width is decreased with increase in activation temperature; this could be possibly due to surfacial

oxidation and deposition of ash or other oxidative products over the pore surface. The BET study confirms that the *Xanthium* derived adsorbent has high micropores volume and thereby has greater adsorption capacity, comparable to standard activated carbons. It is quite clear from the N_2 adsorption studies that the developed *Xanthium* based adsorbent has produced large number of micropores, especially XPT1 is highly micropores in nature. This is attributed to the thermal activation in presence of air, which leads to development of large numbers of new pores. The oxidative activation has held on the surface and interstices of the powdered *Xanthium* samples, leading to char formation, volatilization-devolatilisation and carbon burn-off.

Table 3. Parameters of Langmuir and Freundlich adsorption models for phenol, 2CP and 4CP adsorption on XPT1, obtained from fitting adsorption data at a different temperature.

Adsorbate	Temperature (°C)	Freundlich			Langmuir		
		K_f (mg g^{-1}). (L mg^{-1})$^{1/n}$	1/*n*	R_2^2	q_{max} mg g^{-1}	b L mg^{-1}	R_1^2
Phenol	30	0.745	0.759	0.997	74.083	0.0051	0.999
	40	0.124	0.934	0.999	313.40	0.0003	0.999
	50	0.196	0.759	0.998	200.60	0.0003	0.999

The changes in surfacial morphology have been assessed by SEM method, before and after activation. The SEM images of the untreated *Xanthium*, XPT1, XPT2 and XPT3 are shown in figure 3. The temperature increase in thermal activation is the only parameter for numbers of pores; and

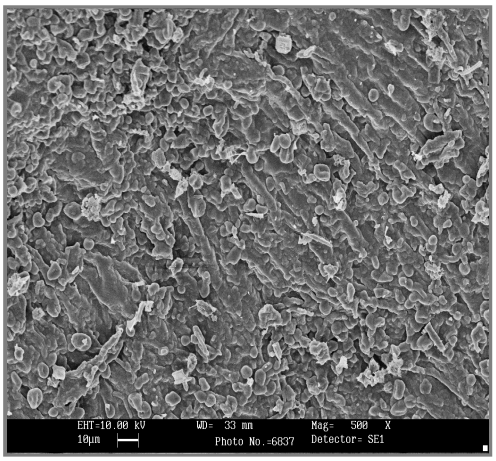

Unactivated *Xanthium* seeds biomass

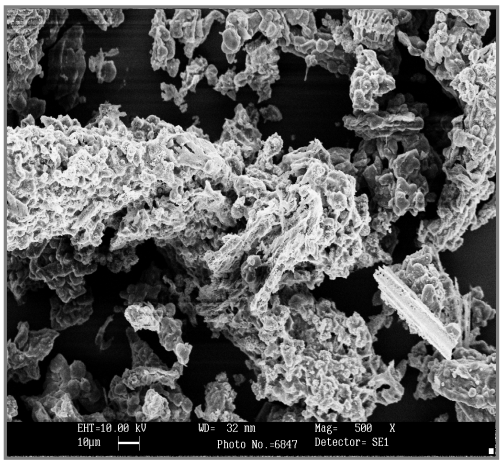

XPT3

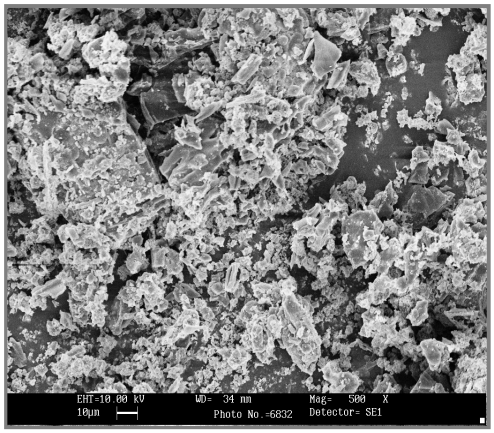

XPT1

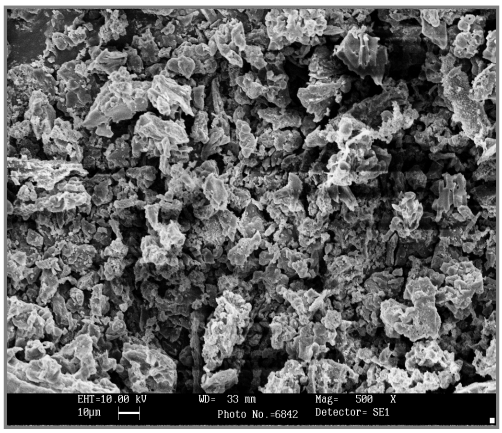

XPT3

Figure 3. SEM images of untreated powdered *Xanthium strumarium* biomass.

reduction in particle size. The emergence of pores and reduction in particle size is quite visible in these figures. The samples have variable particle sizes; but the increase in temperature caused a decrease in the average particle size. The Scanning electron microscopy of the untreated and activated samples was done for different magnifications. The important characteristics of thermal activation are enhancement of pore size and reduction of particle size. The visualization of SEM images confirms the reduction in particle size, development of new pores in material on increasing activation temperature due to volatilization and deposition and devolatilisation leading to restructuring of pore structure affecting pore size and area. The XPT1 sample has reduced particle size and varied pore structures affecting adsorption capacity of the sample.

The Fourier Transform Infra-red spectrum of XPT1 has shown in figure 4. The important peaks observed are of OH group (3750 cm^{-1}), C=C olefinic group (2350 cm^{-1}), C=C aromatic group (broad, 1800-1200 cm^{-1}) and C=O group (750 cm^{-1}) [**24**]. The presence of OH and CO groups on the surface results in its basic nature. The basic surface tends to affect the adsorption behavior of the developed adsorbent, as such surfaces shows preferential adsorption of acidic adsorbates, such as phenolic compounds. The XPT1 material also shows prominent peaks of C=C groups, which shows considerable aromatization that happened in the XPT1 while undergoing thermal activation. The aromatic rings are nonpolar and thereby preferentially attract and attach the nonpolar part of adsorbate, like aromatic ring of phenolic compounds. The X-ray diffraction analysis was done for the XPT1 activated carbon, which was used in removal of phenol. The XRD spectrum shown in figure 5 has a sharp peak at 72.6° and almost otherwise flat plot for XPT1 confirming its amorphous nature [**18**]. A peak at 72.6° was observed for XPT1 which corresponds to SiO_2 [**25**].

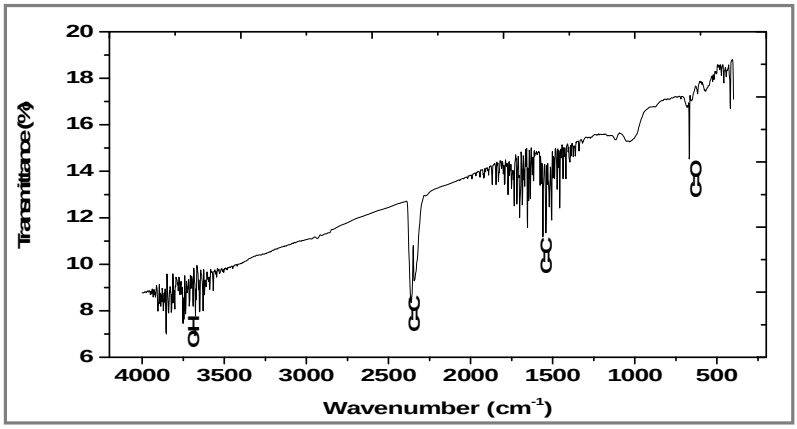

Figure 4. FTIR spectrum of XPT1.

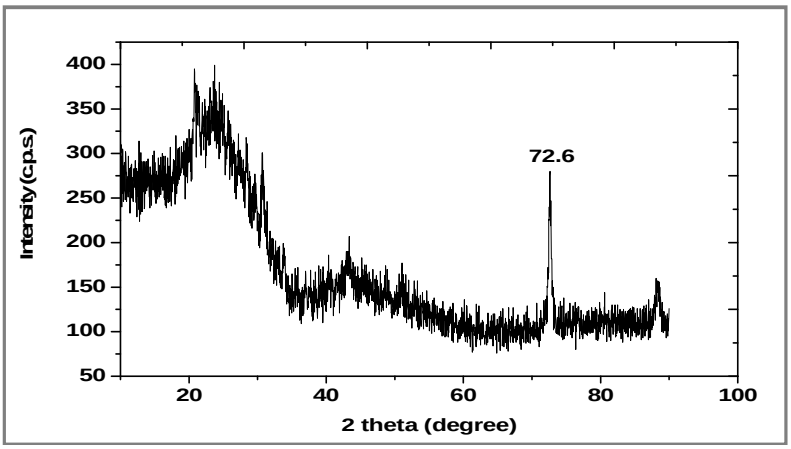

Figure 5. XRD of XPT1.

The activation carbonization leads to polarization of surface, due to development of anionic/cationic charge groups. The surface polarity of XPT1 was assessed in terms of pH_{ZPC}, which is found to be approximately pH=8.7 (figure 6). This shows the surface below pH = 8.7 acquires positively charge and above this pH it acquires negatively charge. The FTIR studies already confirmed the presence of –OH and CO groups on the surface of XPT1. This means in acidic and weakly basic medium (below pH = 8.7), there may be loss of hydroxyl ion or addition of hydronium ion. This confirms the presence of surfacial basic groups, such as OH and CO groups on XPT1. The oxidative activation (in presence of air) enhances the surface oxidation causing the creation of basic groups. The phenolic adsorbate in the current study are acidic in nature (table 1), thus their adsorption is also facilitated by polar interactions. While the adsorption of basic compounds should be less favorable below pH =8.7 [**19**].

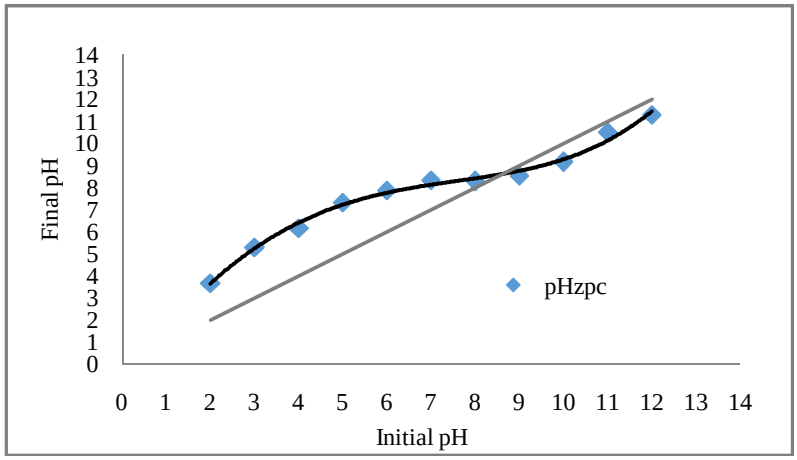

Figure 6. pH_{zpc} for XPT1.

Adsorption studies

Effect of contact time: The adsorption of phenol increases with time in at faster rates on the XPT1 activated carbon as shown in figure 7. The experiment was conducted for more than 5 h, at 30°C with continuous stirring by the use of magnetic stirrer. The XPT1 adsorbent removes about 47.5% phenol from 500 mg L^{-1} solution. There is small variability in adsorption capacity (less than 4%) after 30 min. It is attributed to largely vacant surface sites in the beginning of the experiment [**26**]. Thus 30 min is taken as minimum contact time, to attain maximum adsorption. The maximum adsorption capacity of XPT1 for phenol is found to be 119 mg g^{-1}. The uptake rate of phenolic compounds by XPT1 is much faster than those for other reported adsorbents as in [**18, 26-28**].

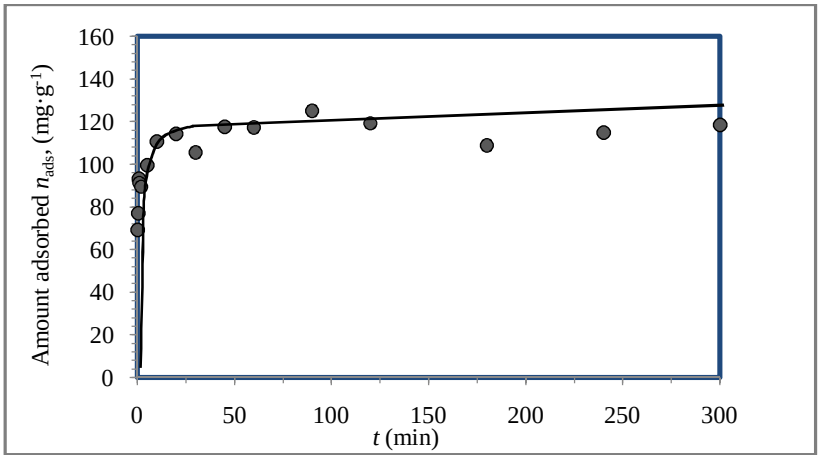

Figure 7. Contact time plot for phenol on XPT1.

XPT1 adsorbent has basic surfacial groups that tend to have negative charge on the surface in the pH range 2 to 8.7 (from pH_{ZPC} experiment); these groups are OH and CO groups as identified in FTIR studies. Phenol has acidic OH group and therefore shows affinity towards XPT1 which is a basic adsorbent. The adsorption of phenol on the activated carbon is influenced by donor-acceptor complex mechanism, as reported in [**18**]. The surfacial carbonyl groups acts as electron donor to the phenolic rings (acceptor). The acidic-basic mechanism supplemented by electron donor–acceptor complexation causes the enhanced adsorption of phenol on the XPT1 bioadsorbent.

Effect of pH: pH of the medium is primary factor which affects the adsorption capacity by controlling the adsorption mechanism and influencing the physiochemical interaction between adsorbent surface groups and adsorbate molecules in their aqueous phase [**26**]. The variation of adsorption capacity of phenolic adsorbates with pH change is reported in figure 8. From contact time experiment, 30 min is taken as the contact (equilibrium) time in this experiment. The pH changes by unit value, from pH 3 to 11. The adsorbent dose is 2 g L^{-1} and adsorbate concentration100 mg L^{-1}. In general, adsorbent adsorbs phenol at each pH value, and the adsorption capacity increases with increase in pH of the solution. There is a rise in adsorption from 7 mg L^{-1} to 20 mg L^{-1} at pH 6 approximately for phenol. The optimum pH condition for adsorption for phenol recorded in this study is approximately pH 7.

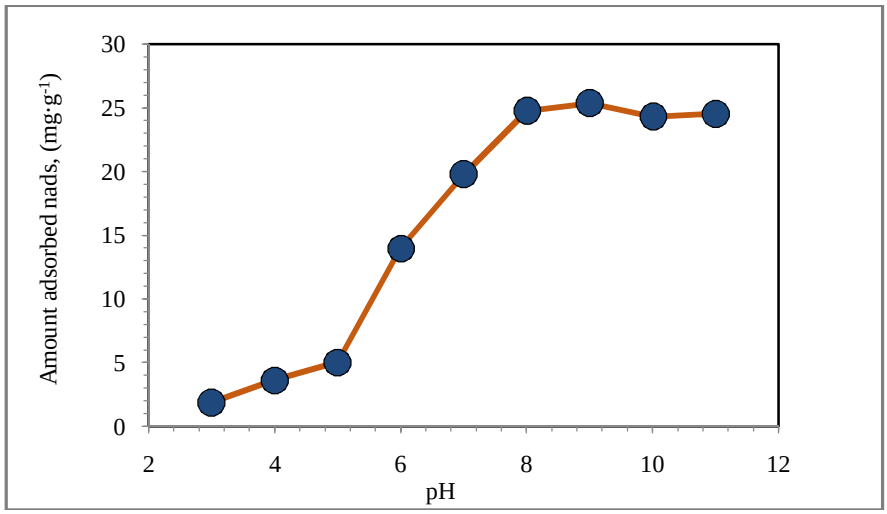

Figure 8. Variation of Adsorption capacity with pH for Phenol on XPT1.

This observed adsorption behaviour can be explained on the basis of proton acceptance (at low pH) and proton donation (at high pH). In acidic solvent phase, protons from acidic solvent competes with phenolic adsorbate and get attached to basic groups of adsorbent, thus decreasing surfacial affinity towards acidic phenol. Second, in strong acidic conditions below pH 4, phenolic adsorbate accept proton from acidic medium and acquire positive charge, limiting its ionization to phenoxide ions. The surface polarity of adsorbate decreases and phenolic ionization decreases with decrease in pH of the aqueous medium. The adsorption under these conditions is governed by physical interactions between phenolic adsorbate and adsorbent. In basic medium, phenolic adsorbates are most likely acidic in nature and thereby have high affinities towards the basic adsorbent surface. The phenolic compounds dissociate to lose proton from hydroxyl group and forms anions. In basic aqueous phase the adsorption is favoured more than desorption in adsorption-desorption equilibrium. The rise in adsorption capacity for phenol is close to pH 6 approximately can be co-related with pK_a values of phenol (table 1). Many other workers reported similar rise in adsorption capacity with increase in pH values.

Effect of concentration and temperature: In figure 9 the dependence of adsorption capacity on initial concentration is shown. The initial concentration of the adsorbate is taken from 20 to 200 mg

L^{1}. The contact time was taken as 30 min and the pH of the adsorbate solution is pH 7. The initial concentration provides the driving force for mass transfer of adsorbate, from aqueous phase to the surface of the adsorbent [29]. Thus adsorption capacity increases with increase in initial concentration [28]. The capacity of adsorbent to remove phenol molecules from aqueous solution increased from 2.08 to 28.48 mg g^{-1} when the initial concentration of phenol solution was increased from 20 to 200 mg L^{-1}. This can be explained on the basis of increase in number of active sites and functional groups with increases in adsorbent dosage [27].

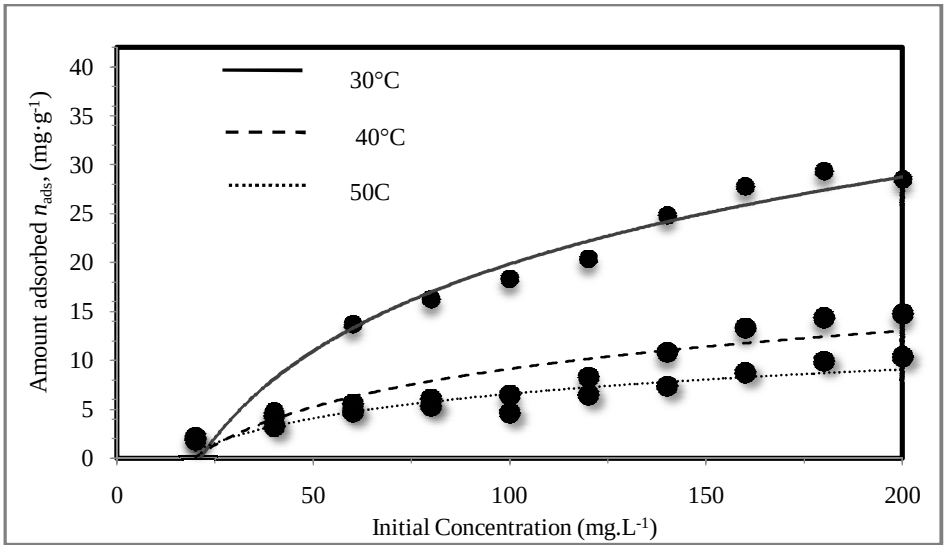

Figure 9. Variation of adsorption capacity with concentration and temperature for phenol on XPT1.

The adsorption capacity is highly influenced by the temperature of the experiment. The increase in temperature causes decrease in adsorption capacity, as higher thermal energy provides activation for desorption processes [30]. The effect of temperature on the adsorption of phenol on the adsorbent XPT1 is shown in figure 9. In is very clear from the figure that at 303 K the adsorption is much higher and regularly increases with increase in initial concentrations. The adsorption capacity decreases with increase in temperature to 313 K and 323 K. The increase in temperature enhances the rate of desorption of phenol from the surface of XPT1.

Adsorption isotherm studies: In order to optimize the adsorption of phenols, adsorption isotherm studies have been conducted at different temperatures (303 K, 313 K and 323 K). Among the various adsorption isotherm equations, fitting of Langmuir and Freundlich isotherms with the experimental data has been tested (table 3). The experimental results: q_{max}, b, R_1^2 (correlation coefficient for Langmuir isotherm), K_f, n, R_2^2 (correlation coefficient for Freundlich isotherm), were presented in table 3. Figure 10 shows the adsorption isotherms of phenolic compounds using XPT1 bioadsorbent with the phenolic adsorbates. The values of R_1^2 and R_2^2 reported for different adsorbates at different temperatures, suggests that in general, both Langmuir and Freundlich models are fitted with the experimental data. In comparison, the experimental data is well fitted to Langmuir model more than Freundlich model, at low temperature 303 K. This suggests the possibility of more extensive mono-layer adsorbate accumulation on XPT1 surface at low temperature. At elevated temperatures the phenolic compounds adsorption is well fitted with both Langmuir and Freundlich models. Thus mono and hetero-layer adsorption takes place on the adsorbent XPT1 surface. The experimental data suggests that at low temperature the adsorption is mostly chemisorptions, and thereby limited to monolayer only. But at higher temperatures desorption takes place at some surface sites, where physiosorption may takes place, resulting in multilayer formation.

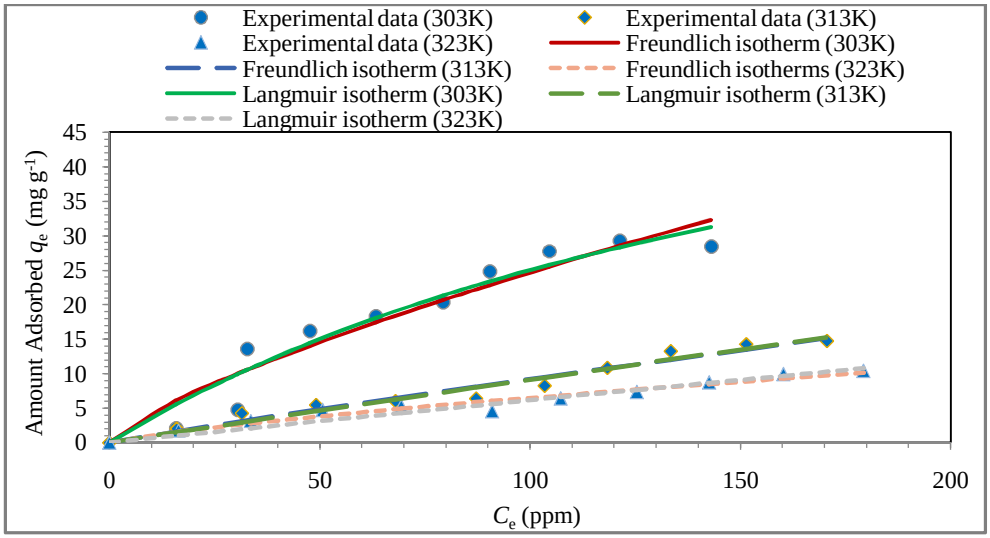

Figure 10. Langmuir and Freundlich isotherm data fitting for Phenol on XPT1.

The rise in temperature has significant impact on adsorption capacity. It is evident from the figure 10 that the extent of adsorption decreases with increase in temperature. This observation is quite obvious as increases in temperature helps to provide activation for the desorption process [**18, 19, 31**]. The Langmuir constant 'b' is related to the affinity of the adsorbent for the adsorbate, values of 'b' for phenol are shown in table 3. At low temperature 303 K, the adsorption capacity of phenol is higher as 'b' is higher at 303 K with increase in temperature, there is decrease in value of 'b' and correspondingly the experimental adsorption capacity decreases at elevated temperatures (313 K and 323 K). This can be explained in terms of forces of attractions between the adsorbate and adsorbate. The chemisorptions is more favourable at low temperature (303 K), resulting in greater adsorption at higher temperature the mode of adsorption changes to mostly physiosorption.

The isotherm shape provides quasi-qualitative information about the solute-surface interactions. The isotherms differentiated on the basis of well accepted classification [**32, 33**]. In this study also the experimental data is found to be best suitably fitted with Langmuir adsorption. On studying the plot in figure 10, it can be easily concluded that the all adsorbates: phenol follows Type L (Langmuir type) adsorption, and the plots typically further classified in type 4 subgroup of L [**16**], showing high concentration of the adsorbates on the XPT1 adsorbent. The Langmuir class (L) plots were obtained for most of the studies of adsorption of phenols. This study confirms that for XPT1 bio-adsorbent, the adsorption of phenols is similar to other previous studies [**26**].

The fitting of adsorption data in Langmuir model can also be confirmed in terms of a dimensionless equilibrium factor R_L, which is defined as:

$$R_L = \frac{1}{1+bC_o} \qquad (4)$$

Where *b* is equilibrium constant and *Co* is initial concentration [**34**]. The R_L values obtained (data not shown) for different adsorbates at different concentrations and temperatures are between 0 and 1, which shows favorable adsorption of phenol on the bioadsorbent XPT1.

In case of fitting of experimental data with Freundlich model, n is a constant which related to adsorbate-adsorbent interactions (adsorption intensity), shown in table 4. The value of $0 < 1/n < 1.0$ shows the favorable adsorbate-adsorbent interactions. The values of 1/n are the range of favorable adsorption for phenol at all temperatures.

APPLICATION

Phenol and its derivatives are toxic by-products of textile industry. The XPT1 bio-adsorbent is useful in efficient and economical removal of phenol from its aqueous phase. This adsorbent can be used in scale-up projects in in-situ removal of phenol and its derivatives.

CONCLUSION

The BET study shows that due to greater activation temperature of 600°C, XPT1 surface has greater micropores leading to greater surface area. The BET surface area, Langmuir surface area, total pore volume, average pore size and average particle size for XPT1 are 1352.82 $m^2 g^{-1}$, 1141153.08 $m^2 g^{-1}$, 1.199 $cm^2 g^{-1}$, 3.54 nm and 4.43 nm respectively. The SEM analysis shows that XPT1 has well developed pores and have least particle size. These studies help to ascertain that XPT1 is porous and can be used as pollutant removal adsorbent. It is confirmed from greater adsorption of methyl orange by XPT1, in comparison with XPT2 and XPT3.

The FTIR of XPT1 shows that it has surfacial OH and CO groups along with olefinic and aromatic groups. The OH and CO groups tend to make XPT1 surface basic in nature. The XRD analysis confirms the amorphous nature of the XPT1 activated carbon. The pH_{ZPC} for XPT1 is about 8.7 this also confirms that the surface of XPT1 bioadsorbent is basic in nature.

The adsorption of phenol on the XPT1 bioadsorbent is found to be favorable due to polar interactions between acidic phenol and basic XPT1 adsorbent. The electron donor CO groups of XPT1, to electron acceptor aromatic ring of phenol also influence the adsorption process. This is confirmed by higher extent of adsorption of phenol, with lesser adsorption contact time. The contact time experiment gives the optimum contact time of 30 min, which is found to be least as compared to other related studies for phenol. The phenolic removal is about 47.5% from original 500 mg L^{-1} solution, the adsorption capacity is found to be 119 mg g^{-1}. The pH of the experiment is found to be important factor in deciding the extent of adsorption. In acidic conditions the adsorption capacity of XPT1 for adsorption of phenol is lesser, but with increase in pH, the adsorption capacity increases. The optimum pH is found to be close to pH 7. The adsorption extent also depends on the initial concentration and temperature of the experiment. The adsorption capacity increases from 2.08 to 28.48 mg g^{-1} when the initial concentration of phenol solution was increased from 20 to 200 mg L^{-1}. The extent of adsorption is higher at 303 K, as compared to other experimental temperatures (313 K and 323 K).

The adsorption isotherm between XPT1 adsorbent and phenol adsorbate follows Langmuir adsorption model at low temperature (303 K), but as the temperature increases isotherm data is well fitted with both Langmuir and Freundlich models. Thus monolayer adsorption is more prominent at low temperature adsorption suggesting preferential chemisorptions at low temperature. But at higher temperatures the adsorbate-adsorbent interaction is preferentially physical in nature, thereby multilayer adsorption predominates. The isotherm shape is typically Langmuir type L adsorption. The R_L values also confirm the adsorption mechanism between phenol and XPT1 follows Langmuir model.

REFERENCES

[1]. Q. Liu, T. Zheng, P. Wang, J. Jiang, and N. Li, Adsorption isotherm , kinetic and mechanism studies of some substituted phenols on activated carbon fibers, **2010**, 157, 348-356.
[2]. J. R. Rao, T. Viraraghavan, Biosorption of phenol from an aqueous solution by Aspergillus niger biomass, **2002**, 85, 165-171.
[3]. P. Girods *et al*, Activated carbons prepared from wood particleboard wastes : Characterisation and phenol adsorption capacities, **2009**, 166, 491-501.

[4]. P. S. Nayak, B. K. Singh, Removal of phenol from aqueous solutions by sorption on low cost clay, **2007**, 207, 71-79.
[5]. G. Ruiying, W. Jianlong, Effects of pH and temperature on isotherm parameters of chlorophenols biosorption to anaerobic granular sludge, **2007**, 145, 398-403.
[6]. K. P. Singh, A. Malik, S. Sinha, P. Ojha, Liquid-phase adsorption of phenols using activated carbons derived from agricultural waste material, **2008**, 150, 626-641.
[7]. J. Huang, X. Wang, Q. Jin, Y. Liu, Y. Wang, Removal of phenol from aqueous solution by adsorption onto OTMAC-modified attapulgite,. *Environ. Manage.*, **2007**, 84(2), 229-236.
[8]. R. Kumar, Groundnut shell powder as low cost Natural adsorbent for total chromium in spent chrome liquor, *J. Applicable. Chem.*, 2017, 6(5), 841–845.
[9]. R. Pagutharivalan, N. Kannan, Plant waste-Economical adsorbent for the removal of cationic dye from aqueous solution, *J. Applicable Chem.*, 2018, 7(1), 103–111.
[10]. S. Sagar, A. Rastogi, Biosorption of Methylene blue from aqueous solutions by using blue green algae Oscillatoria sp. :Kinetic and equilibrium studies, *J. Applicable Chem.*, **2017**, 6, 3, 374–384.
[11]. P. K. Gautam *et al*, Preparation of activated carbon from Alligator weed (Alternenthera philoxeroids) and its application for tartrazine removal: Isotherm, kinetics and spectroscopic analysis, *J. Environ. Chem. Eng.*, **2015**, 3(4), 2560-2568.
[12]. R. K. Gautam *et al.*, Removal of tartrazine by activated carbon biosorbents of Lantana camara: kinetics, equilibrium modeling and spectroscopic analysis, *J. Environ. Chem. Eng.*, **2015**, 3(1), 79-88.
[13]. S. Khamparia, D. K. Jaspal, Xanthium strumarium L. seed hull as a zero cost alternative for Rhodamine B dye removal, *J. Environ. Manage.*, **2017**, 197, 498-506,.
[14]. S. Khamparia, D. K. Jaspal, Evaluation of decoloration potential of Xanthium Strumarium seed hull for adsorption of Direct red 81 in aqueous solution, *Environ. Dev. Sustain.*, **2017**, 19(5), 1933–1951.
[15]. C. K. Jain, D. S. Malik, A. K. Yadav, Applicability of plant based biosorbents in the removal of heavy metals: a review, *Environ. Process.*, **2016**, 3(2), 495-523,.
[16]. A. Dąbrowski, P. Podkościelny, Z. Hubicki, M. Barczak, Adsorption of phenolic compounds by activated carbon-a critical review, *Chemosphere*, **2005**, 58(8), 1049-1070.
[17]. O. Ioannidou, A. A. Zabaniotou, Agricultural residues as precursors for activated carbon production-A review, **2007**, 11, 1966-2005.
[18]. A. Bhatnagar, Removal of bromophenols from water using industrial wastes as low cost adsorbents, **2007**, 139, 93-102.
[19]. V. K. Saini, S. Suthar, C. Karmveer, K. Kumar, Valorization of Toxic Weed Lantana camara L . Biomass for Adsorptive Removal of Lead, **2017**, 1-12.
[20]. O. Hamdaoui, E. Naffrechoux, Modeling of adsorption isotherms of phenol and chlorophenols onto granular activated carbon Part I. Two-parameter models and equations allowing determination of thermodynamic parameters, **2007**, 147, 381-394.
[21]. T. Nargawe, A. K. Rai, R. Ameta, S. C. Ameta, Adsorption study for removal of crystal violet dye using MMT-MWCNTs composite from aqueous solution, *J. Applicable Chem.*, **2018**, 7(5), 1252–1259.
[22]. M. Ahmedna, W. E. Marshall, A. A. Husseiny, R. M. Rao, The use of nutshell carbons in drinking water filters for removal of trace metals, **2004**, 38, 1062–1068.
[23]. D. Savova *et al.*, Biomass conversion to carbon adsorbents and gas, *Biomass and Bioenergy*, **2001**, 21(2) 133–142.
[24]. R. Arumugam, P. Periakaruppan, A green and facile one-pot synthesis of Ag NPs using *Bombax pendantrum* leaf extract for effective removal of organic dyes, *J. Applicable Chem.*, **2018**, 7(6), 1534–1546.
[25]. R. Azargohar, A. K. Dalai, Biochar as a precursor of activated carbon, *in Twenty-Seventh Symposium on Biotechnology for Fuels and Chemicals*, **2006**, 762–773.

[26]. M. Achak, A. Hafidi, N. Ouazzani, S. Sayadi, L. Mandi, Low cost biosorbent 'banana peel' for the removal of phenolic compounds from olive mill wastewater: kinetic and equilibrium studies, *J. Hazard. Mater.*, **2009**, 166(1), 117–125.
[27]. M. H. Al-malack, M. Dauda, Journal of Environmental Chemical Engineering Competitive adsorption of cadmium and phenol on activated carbon produced from municipal sludge, *J. Environ. Chem. Eng.*, **2017**, 5(3), 2718–2729.
[28]. A. Kumar, H. M. Jena, Removal of methylene blue and phenol onto prepared activated carbon from Fox nutshell by chemical activation in batch and fi xed-bed column, *J. Clean. Prod.*, **2016,** 137, 1246–1259.
[29]. E. O. Oyelude, J. A. M. Awudza, S. K. Twumasi, Removal of malachite green from aqueous solution using pulverized teak leaf litter : equilibrium , kinetic and thermodynamic studies, *Chem. Cent. J.*, **2018**, 1-10.
[30]. J. C. Thermodynamics, B. Taraba, and P. Bulavová, Adsorption enthalpy of lead (II) and phenol on coals and activated carbon in the view of thermodynamic analysis and calorimetric measurements," *J. Chem. Thermodyn.*, **2018**, 116, 97-106.
[31]. S. Cengiz, L. Cavas, Removal of methylene blue by invasive marine seaweed : Caulerpa racemosa var . cylindracea, **2008**, 99, 2357-2363.
[32]. C. H. Giles, D. Smith, A. Huitson, A general treatment and classification of the solute adsorption isotherm. I. Theoretical, *J. Colloid Interface Sci.*, **1974**, 47(3), 755-765.
[33]. C. H. Giles, A. P.D'Silva, I. A. Easton, A general treatment and classificationof the solute adsorption isotherm, II. Experimental interpretation., *J. Colloid Interface Sci.*, 1974, 47, 766–778.
[34]. N. S. Rajurkar, Novel adsorbents for waste water treatment, *J. Applicable Chem.*, **2018**, 7 (6), 1526–1533.